ASSOCIAZIONE NAZIONALE ITALIANA DI INGEGNERIA SISMICA
ANIDIS
Italian National Association of Earthquake Engineering

XVIII CONVEGNO ANIDIS
L'ingegneria sismica in Italia
ASCOLI PICENO 2019
15-19 Settembre

Site effects on analytical fragility curves of bridge piers

Alessandra De Angelis[a], Maria Rosaria Pecce[a], Stefania Sica[a]
[a] *Dipartimento di Ingegneria, Università degli studi del Sannio, Piazza Roma 21, 82100 Benevento, Italy*

Keywords: bridge piers; fragility curve; site effects.

ABSTRACT
In seismic areas, bridges and road infrastructures are of paramount importance to ensure prompt transportation and emergency management during and after strong earthquakes. Fragility functions, which define the structural damage probability under different ground shaking levels, could be very useful to assess the seismic performance of bridges and their components. Field evidence from past earthquakes occurred worldwide indicates that local soil conditions may affect the overall seismic performance of bridges. The paper investigates the effects of seismic site response on the development of analytical fragility curves for reinforced-concrete bridge piers. In the first part of the paper, a detailed literature review is illustrated to gain the current knowledge on fragility function development in terms of computational methods, intensity measures, damage states and indexes.
For a bridge case-history, representing a quite common configuration in Italy, seismic fragility relationships were later calculated after performing specific site response analyses, which provided the proper input ground motion at the base of the piers. Bridge pier damage indexes were finally obtained by performing time-history analyses.

1 INTRODUCTION

In a transportation system, bridges are among the key elements to assure network operation during and after a strong earthquake. Unfortunately, worldwide past earthquakes highlighted the inner vulnerability of bridges, with failures that caused huge human and economic losses. Actually, many existing bridges have been designed to resist only to gravity loads and, if maintenance is not efficient and accurate, the seismic risk associated to the road infrastructure may be very high. In order to improve life safety and reduce the economic losses, it is important to quantify the risk itself and define priority of intervention for its mitigation.

Bridge damage caused by past earthquakes was observed to span from light to collapse level (Shinozuka and Banerjee 2005). The five most probable failure mechanisms in girder bridges may be summarized as: formation of plastic hinge at the base of the pier, large relative displacements with pounding between two adjacent decks at expansion joints and abutments or unseating of the deck with consequent fall, failure of the restraints at the abutments and expansion joints, premature shear failure in columns, liquefaction of the surrounding soil.

Padgett and Des Roches (2006) underlined that the abutments are other crucial components that may be vulnerable for multi span simply or continuous girder bridges. Therefore, the transverse deformation in the abutment could be chosen as a response parameter.

In recent years, fragility curves have been proposed as a useful tool for the assessment of the seismic risk of many types of buildings (Rossetto and Elnashai, 2003; Kappos et al., 2006). These relationships actually give the likelihood that a structure will meet or exceed prefixed levels of damage for a given intensity of the seismic action. Fragility curves have been proposed also for bridges (Hwang et al., 2001).

Conceptually, fragility functions can be referred to classes of structures or to a single structure that is considered as representative of a given typology. In all cases, however, they can be used for risk analysis at large scale to address the resources for future interventions. In this paper, the approaches proposed in literature for developing fragility curves of bridges are firstly recalled. With reference to a specific case-study, emphasis is later given to the role exerted by local

soil conditions (site effects) in defining the ground motion to be applied at the base of the bridge pier. The selected bridge is characterized by a pier made of two circular columns. For this bridge type, the seismic damage is likely to occur with plasticization at the pier base and the damage parameter is the plastic rotation. To develop the fragility functions of the bridge pier, seismic site response analyses have preliminary been carried out and the computed free-field ground motion adopted as input signals for the structural analyses. This procedure allows nonlinear soil response under different shear strain levels (induced by the earthquake) to be taken into account. At this stage of the work, however, the kinematic interaction occurring between the soil and the pier foundation (pile group) has been ignored. As well-known, the effect of kinematic interaction between the foundation and the surrounding soil generally consists in reducing the motion transmitted to the superstructure. This modification depends on several factors, such as the frequency range of the input motion, pile diameter and soil stiffness. In literature, some closed-form solutions to switch from the free-filed ground motion to the foundation input motion are provided for very simple soil types (homogeneous half-space or two-layered soil). In these simplified hypotheses, it was found that with reducing soil stiffness or with increasing the frequency content of the signal or pile diameter, higher difference between the free field and the foundation input motion might occur (Fan et al., 1991, Di Laora & de Sanctis, 2013).

2 FRAGILITY ANALYSIS OF BRIDGES

Fragility relationships are defined as the conditional probability that a structure will meet or exceed a certain level of damage for a given ground motion intensity. Fragility curves may be developed for structural components as well as for the structure itself as a unique system. Component fragility curves are useful to identify weak parts of the structure while system fragility curves are used in seismic risk assessment.

Generally, fragility curves can be developed using expert opinion (ATC 1985), empirical data from past earthquakes, and analytical methods through nonlinear dynamic analysis or quasi static analysis. In particular, the expert-based fragility curves, relying on the experience of a number of experts, were developed in the Eighties and they represent the first example of fragility analysis. Due to the availability of damage data collected during several past earthquakes (Loma Pietra 1989, Northridge 1994 and Kobe 1995), expert-based fragility curves were replaced by empirical curves developed through statistical analysis of post-earthquake inspections (Basöz et al. 1998; Yamazaki et at. 1999; Shinozuka et al. 2000). The most important limitation of the empirical curves is the lack of a functional link with ground motion levels. To overcome this limitation, analytical fragility curves were developed through nonlinear dynamic analysis or quasi-static analysis in order to assess bridge vulnerability. It is thus possible to perform fragility analysis for a specific region and also for regions where there is no history of past earthquakes. Hwang et al. (2001), Choi (2002), and Choi et al. (2004), for instance, generated analytical fragility curves for bridges in Central and Southeastern America. Other researchers, instead, investigated the seismic fragility of typical multispan continuous and simply supported highway bridges in New York State (Pan 2007 and Pan et al. 2010). Ramanathan (2012) developed fragility curves for typical Californian bridge classes while Tavares et al. (2012) and Billah and Alam (2013) developed seismic fragility curves for highway bridges in eastern and western Canada, respectively.

For the generation of fragility curves, simplified and more detailed procedures have been developed (Mander and Basöz 1999, Mackie and Stojadinović 2001, Karim and Yamazaki 2003, Gardoni et al. 2003).

Most of the studies regarding bridge fragility curves are focused on as-built bridges. The effect of different retrofit strategies such as carbon fibre jacketing and viscous damper, steel jacket, concrete jacket, Carbon Fiber Reinforced Polymer (CFRP) jacket, has recently been evaluated by different authors (Agrawal et al. 2012, Billah et al. 2013, Stefanidou and Kappos 2013).

During earthquakes bridges could be affected by Soil-Structure Interaction (SSI). Actually, the relative stiffness between the bridge piers and the soil–foundation system could dictate such interaction (Chaudhary et al. 2001, Gerolymos & Gazetas, 2006, Mucciacciaro et al. 2018). By tradition, the seismic analysis of bridges has been performed disregarding SSI. Nowadays, it is

definitely well known that in some cases a misleading response for bridge components and for the overall system could be attained if SSI is not accounted for.

In literature, a few studies contemplating SSI in bridge models can be found (Morici et al. 2019, González et al. 2019). Some authors (Saadeghvaziri et al. 2000, Stefanidou 2018), Aygün 201, Mwafya et al. 2010) studied the SSI effects on the bridge response using equivalent translational and rotational springs. A full 3D bridge-foundation system was proposed by Elgamal et al. (2008), Zong (2015) and by Jeremić et al. (2009), who considered also layered soil deposits.

Fragility curves accounting for SSI were developed and discussed by Kwon and Elnashai (2010) comparing different modelling strategies of the abutment and of foundation system (fixed-base assumption, structure on lumped springs from literature solutions, lumped springs from 3D FE analyses and Multiplatform 3D FE models).

The effect of liquefiable soils on fragility curves of a multi-span continuous steel bridge has been addressed by Aygün et al. (2011) and Bowers (2007).

3 CASE STUDY: SEISMIC FRAGILITY ANALYSIS OF A TYPICAL EUROPEAN BRIDGE

3.1 Typical bridges in the European Area

Kaundinya and Heimbecher (2011) collected the different typologies of bridges existing in Europe. They identified and categorized through major construction specifications (e.g. length, material, etc.) the bridges on the main highways of the Trans European Road Network. In total, 38 different bridge types were identified as relevant in the EU including girder bridges, integral bridges, arch bridges, cable stayed bridges, suspension bridges, truss bridges and others. Based on the data mentioned above, the most recurrent bridge type in Europe is the so-called "girder bridge", either simply supported or continuous with different superstructure types. More than 64 % of all bridges in the countries participating to the survey are built as a single span or continuous girder bridge. Girder bridges are used for short (< 30 m) and medium (< 75-100 m) span bridges. The most common material used for bridges in Europe is reinforced and pre-stressed concrete (86%). Moreover, most of the bridges with short spans (<30 m) are built using concrete as the main construction material. Medium span bridges (30–100 m) often are composite constructions (steel superstructure with concrete deck/pavement) or pure steel structures.

The most recurrent spans among the European bridges are the short ones (<30 m), reflecting the large number of small bridges in the road network. For this reason, in the paper a multi-span simply supported girder bridge with pre-stressed beams resting on framed piers has been considered to carry out fragility analysis.

3.2 Bridge and Modelling

The geometry of the selected bridge is shown in Figure 1. The bridge consists of 3 spans with a length of 25 meters The deck consists of 4 prestressed concrete girders equally 3m spaced and a slab 0.2 m thick made of cast-in-place concrete. The girders are supported on piers realized with two-column bents. The concrete column bent consists of an inverted T-shape section cap beam and two columns 9 m high with a diameter of 1.5 m. Each column is reinforced by 23ϕ20 vertical bars and ϕ10 spiral hoops spacing 200 mm. The column bents are supported on a 2x2 pile group (4 cast- in-place piles, 16 meters long with a diameter of 1.25 meter). The cross sections of the column and the cap beam are shown in Figure 1. The material used for the bridge pier is concrete with nominal compressive strength f_{ck}=25 MPa and steel reinforcement with tensile strength f_{yk}=430MPa.

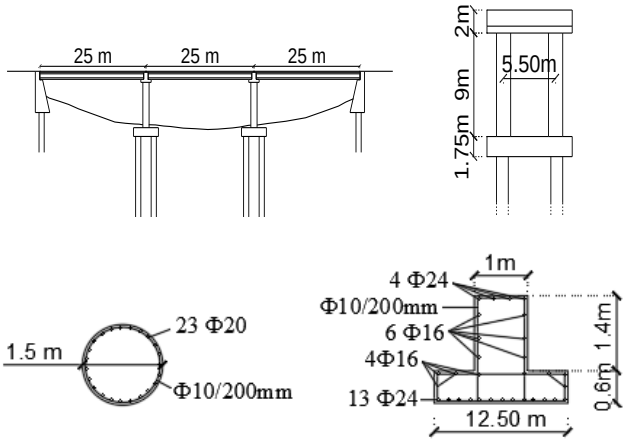

Figure 1. Configuration of the analysed bridge

In Figure 2 it is shown the numerical model developed to analyse the selected case study. The deck and the prestressed concrete girder are combined together and modeled as elastic beam

elements. Parameters that can be considered as random variables are set to their mean values for developing a basic bridge model as better explained in section 4.4.

The columns of the pier are modeled as frame elements with lumped plasticity at the ends. For this type of bridge, plastic hinges can only form at the ends of the columns, as pinned joints with bearings that can accommodate rotations between the cap beam and the girders. The nonlinearity of the whole pier has been modelled by a moment-curvature relationship as reported in Pan et al. (2007). The constitutive relationship of Mander (1988) has been assumed for the concrete in compression neglecting the confinement effect. An elastic-plastic behaviour has been considered for the reinforcement steel.

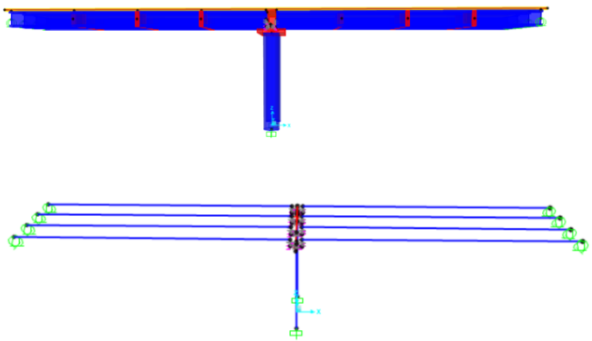

Figure 2. Bridge model

The moment-curvature relationship adopted for the pier section is shown in Figure 3. The nonlinear behavior of the column section can be idealized as an elastic-perfectly-plastic bilinear model, defining the curvature at the yield point ϕ_y and the ultimate curvature ϕ_u.

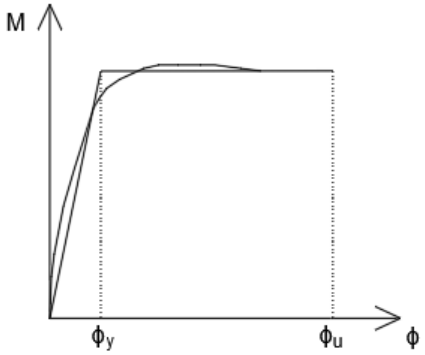

Figure 3. Moment-curvature relationship for the piers

Assuming a constant curvature over the length of the plastic hinge (L_p), the plastic rotation can be calculated as $\theta_p = \phi \cdot L_p$ where L_p is calculated according the formulation suggested by the NTC2018:

$$L_{pl} = 0.1L_v + 0.17h + 0.24\frac{d_{bL}f_y}{\sqrt{f_c}} \qquad (1)$$

In eq. (1), L_v is the shear length, that is the distance between the sections of zero and maximum bending moments, and d_{bL} is the diameter of a longitudinal reinforcing bar.

A rigid-plastic moment- rotation relationship is assumed for the plastic hinge and introduced in the SAP2000 model.

Due to the symmetry of the structure, the seismic analysis can be performed independently in the two horizontal directions

3.3 Input signal selection

In seismic reliability assessment of structures, a relationship between ground motion intensity and structural response needs to be researched. In other words, the goal of the structural analysis is to estimate the response of the structure under input motions having specified intensities so that the conditional probability of exceeding a certain limit state may be calculated. The structural response is highly dependent on the set of input signals selected for the analysis. As underlined by Baker and Cornell (2006), the use of ground motion records with different spectral shapes can substantially modify the collapse capacity as much as 70%. An appropriate selection of ground motion recordings, hence, is a key issue in fragility function assessment. For such an aim, various levels of ground motions should be considered to evaluate the probability that the bridge will be subjected to certain damage state within a given return period. It is worth pointing out that the set of input signals should not only account for the seismic hazard but also for local soil conditions (Silva et al., 1988). As well-known, recordings at the bedrock may strongly be modified in frequency and amplitude by the upper soil layers. If a bridge is not founded on rock, the input signals should account for seismic site effects, which are strongly dependent on soil nonlinearity mobilized by the earthquake.

For a proper selection of the input signals to be adopted for assessing fragility curves of bridge piers, the following two approaches have been hereinafter adopted:

– *Approach A - Generation of Acceleration Time Histories Based on the Design Spectra:*

In this approach a target spectrum is used to select an appropriate set of ground motions,

which are representative of site seismicity. Scaled natural records are matched and compared to a target spectrum over a certain range of periods. This range should include the important modes of the structure, considering also the period elongation due to the inelastic deformation of the structure. A period range from 0.2 to 2 times the first period of the structure is recommended for this purpose. A set of seven accelerograms has been selected with the REXEL software (Iervolino et al. 2009) through a procedure that takes into account the seismogenic characteristics of the area and their compatibility with the identified soil category (Figure 4). For the case at hand, it is assumed that the bridge is located in a medium seismic hazard region characterized by a peak ground acceleration of 0.3 g. Other features of these records are: (i) moment magnitude range: 4.3–6.3, (ii) hypocentral distance less than 30 Km, and (iii) soil category C according to NTC2018.

For fragility curve generation, various levels of ground motion should be considered. In this study, the following hazard levels were taken into account: 0.1g, 0.2g, 0.3g, 0.4g, 0.5g, 0.6g, 0.7g and 0.8g.

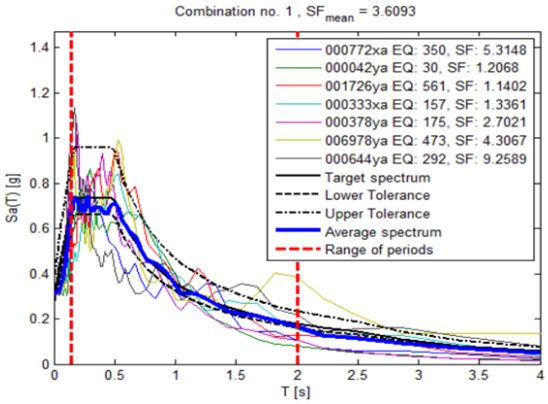

Figure 4. Set of seven spectrum-compatible accelerograms on soil type C.

– *Approach B - Generation of Acceleration Time Histories by Site Response Analysis*

The ground motion at the base of the piers was obtained by performing specific site response analyses through the software EERA (Bardet et al., 2000). An upward seismic wave propagation was simulated accounting for the actual stratigraphy of the soil deposit and nonlinear soil behaviour under cyclic loading (i.e., shear stiffness degradation and damping increase with the mobilized shear strain). The bedrock depth (Vs>800 m/s) was identified around a depth of 100 m below the ground level. For each layer of the soil deposit, Table 1 reports thickness, depth, unit weight γ and the shear wave velocity V_S provided by in-situ SASW tests. As the nonlinear soil behaviour regards, the decay of the shear modulus G and the increase of the damping ratio D with the shear strain, γ, were calibrated on laboratory data provided by Seed & Idriss (1970) for coarse-grained soils and by Vucetic & Dobry (1991) for clays (plasticity index PI=15%) (Figure 5).

Table 1. Main properties of the soil deposit.

Deep [m]	Thickness [m]	Soil typology	γ [kN/m^3]	Vs [m/s]
0-0.5	0.5	sandy gravel	18.50	95
0.5-2.5	2.0	gravel with sand	18.50	180
2.5-5	2.5		18.50	240
5-8	3.0		18.50	275
8-12	4.0		18.50	215
12-30	18.0	sandy silt with gravel	18.50	250
30-50	20.0		18.50	330
50-70	20.0		20.00	500
70-90	20.0		20.00	600
90-100	10.0		20.00	650
100-	-	Bedrock	20.00	800

Since the fragility functions are obtained by increasing the seismic motion at the base of the structure, this procedure requires a contextual simulation of the nonlinear phenomena mobilized in the soil layers. In the approach B proposed in this study, to avoid scaling too much a unique set of 7 accelerograms, with the counterpart of having unrealistic seismic signals (it is advisable not adopting scaling factors higher than 2.5), three different sets of 7 accelerograms recorded on rock outcrop (soil type A) have been researched through the software REXEL v3.5, corresponding to the following PGA values at the site:

- 0.224g (PGA on rock outcrop for a structure life equal to 50 years and limit state SLV Tr=475 y);

- 0.396g (PGA on rock outcrop for a structure life equal to 100 years and limit state SLV Tr=949 y);
- 0.55g (PGA on rock outcrop for a structure life equal to 100 years and limit state SLC Tr=1950 y);

For seismic hazard levels corresponding to PGA of 0.1g and 0.8g, reference was made to the two sets of natural accelerograms found for PGA=0.224g and PGA=0.55g, respectively. The original signals were scaled in amplitude with a scaling factor less than 2.5. In short, five sets of 7 accelerograms (total amount of 35 accelerograms) were adopted for the fragility curve assessment of the selected bridge pier.

Figure 6 shows the profile of the measured shear wave velocity Vs (linked to the initial shear stiffness G_{max} of the soil layer) and the numerical values corresponding to the mobilized shear moduli ($G_{mob}<G_{max}$), which were derived from the linear equivalent site response analyses (S.R.A.). In short, a single S.R.A. velocity profile in Figure 6 corresponds to the average of 7 predictions for each accelerogram set.

Figure 7 (a-c) shows the mobilized shear modulus and damping ratio for signals having on rock outcrop PGA of 0.224g, 0.55g and 0.8g, respectively. It can be observed that with increasing the PGA of the input signals, the shear modulus of the soil deposit is decreased up to 40% of the initial value Go while the damping ratio is increased up to 18%. In a future stage of the work, these modified values of soil shear stiffness and damping ratios will be adopted to evaluate the impedance functions at the base of the pier to account for SSI effects on the fragility curves.

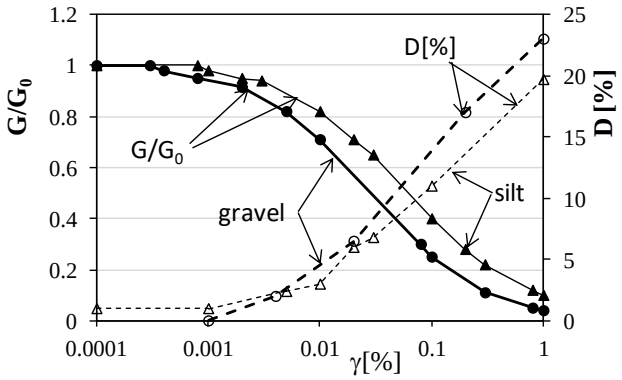

Figure 5. G/G_0-γ and D-γ curves assigned to the soil layers.

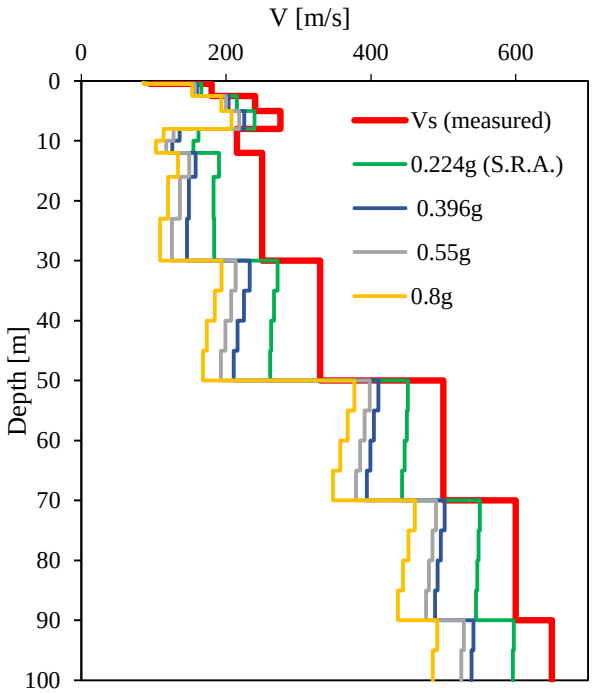

Figure 6. Initial and mobilized shear wave velocity.

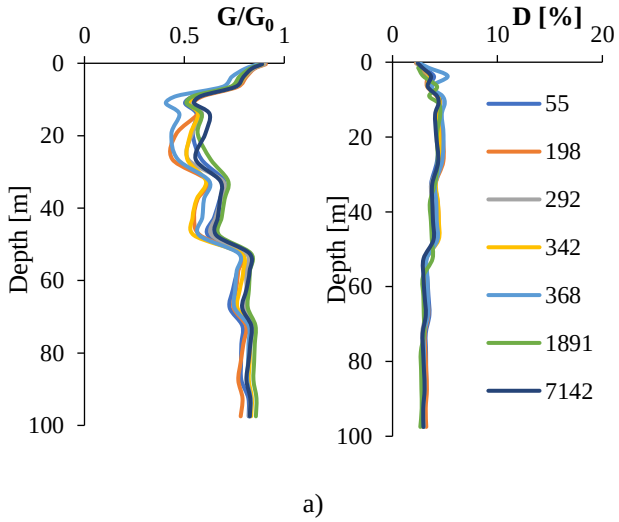

a)

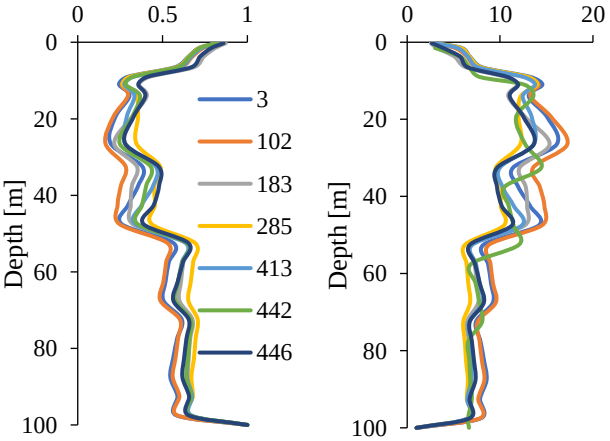

b)

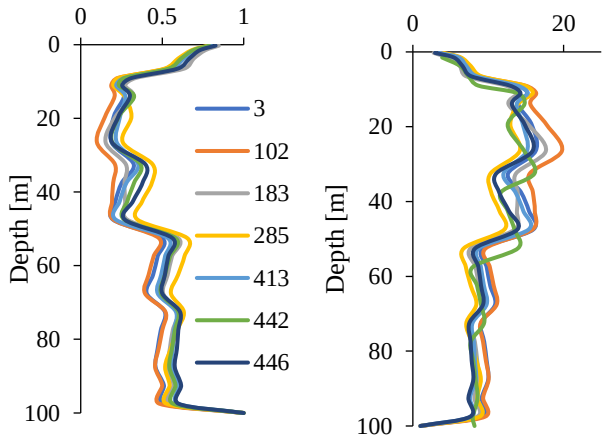

c)

Figure 7. Shear modulus and damping ratio profiles obtained by S.R.A. with the accelerogram sets having on rock outcrop PGA of 0.224g (a) and 0.55 g (b) and 0.8g (c). The numbers in the legend identify the seismic signal code.

4 FRAGILITY CURVES

Seismic fragility analysis of the selected bridge was carried out by considering uncertainties in concrete compressive strength and reinforcement yield strength. Probability distributions were assumed for each parameter, and the probability density function of each random variable was divided into a histogram with equal probability intervals so that the corresponding cumulative distributions was graded linearly. For the concrete compressive strength of the case at hand, a normal distribution was assumed. The mean value of the strength is 41 MPa and standard deviation is 4.24 MPa (COV=0.10). Conversely, for the yield strength of reinforcing steel, a lognormal distribution was assumed. The nominal strength is 385 MPa while the standard deviation is 42 MPa (COV=0.11).

Probability distributions of each variable can be divided into a number of regions of equal areas. Assuming 5 ranges of probability distributions for the concrete and 3 ranges for the steel, 15 bridge models were figured out. Note that a sample bridge model with uncertainties in these parameters can be developed by selecting one of the ranges for each of the random variables randomly. Each of the fifteen bridge models are paired with 7 ground motions to generate 105 (7x15) bridge-earthquake pairs for the structural demand analysis.

Statistical data on structural demand corresponding to peak ground accelerations (PGAs) from 0.1g to 0.8 g were generated through structural analysis of the bridge-earthquake pairs. The capacity of the pier was determined from the analytical model for a particular level of damage. The pier is usually damaged in flexure under seismic actions. Therefore, only flexure capacity analyses of the piers were carried out in this study.

Two different levels of pier damage (limit states) corresponding to the two curvature thresholds ϕ_y and ϕ_u were identified.

The fragility is defined as the conditional probability that a certain random variable will meet or exceed a predefined value under a given condition as stated in equation (2).

$$P_f = P\left[\frac{S_d}{S_c} \geq 1\right] \quad (2)$$

where P_f is the failure probability for a specific damage state, S_d and S_c are the structural demand and structural capacity, respectively. It should be noted that equation (2) only defines value for the probability under a certain seismic load because the bridge demand (S_d) depends on earthquake ground motion intensity.

Typically, the random natures of both S_d and S_c are described by a lognormal probability distribution. Hence, fragility P_f can be expressed as a standard normal distribution here reported (Eq. 3).

$$P_f = \phi\left(\frac{ln(S_d/S_c)}{\sqrt{\beta_d^2+\beta_c^2}}\right) \quad (3)$$

where S_c is the mean value of the structural capacity defined for the damage state, β_c is the lognormal standard deviation of the structural capacity, S_d is the mean value of seismic structural demand in terms of a chosen ground motion intensity parameter, in this case, PGA, and βd is the lognormal standard deviation of the structural seismic demand.

Several methods may be adopted to obtain the structural demand, such as the elastic response spectral analysis, nonlinear static analysis and nonlinear time history analysis. In this work, nonlinear time history analyses were carried out to obtain structural seismic demands for earthquakes of different PGAs. By performing nonlinear time-history analysis for each of the bridge-earthquake pair, the maximum response of the bridge pier rotations was obtained. Ratios of structural demand and capacity (S_d/S_c) were obtained by dividing peak structural demands by

corresponding capacities (i.e. θ/θ_y for the first damage state and θ/θ_u for the second damage state).

Since the PGAs of the selected accelerogram set vary from 0.1g to 0.8 g, the ratio S_d/S_c can be plotted as a function of PGA. As stated above, the structural demand (S_d) and the structural capacity (S_c) follow lognormal distribution (Shinozuka et al., 2000; Hwang et al. 2001). It can be assumed that $\ln(S_d/S_c)$ follows a normal distribution versus ln(PGA). The relationship between $\ln(S_d/S_c)$ and ln(PGA) can be obtained through regression analysis of 120 data points obtained through nonlinear time history analyses.

The fragility for a specific damage state can be determined as:

$$P_f = P\left[\frac{S_d}{S_c} \geq 1\right] = 1 - \phi\left(\frac{\ln(1)-\lambda}{\varepsilon}\right) = \phi\left(\frac{\lambda}{\varepsilon}\right) \qquad (4)$$

where λ and ε are the mean and standard deviation of $\ln(S_d/S_c)$ obtained from the regression analysis. The parameter λ in Eq. (4) is expressed as a function of PGA through regression analysis. The standard deviation ε is a value obtained from the response and capacity data. Hence, the effects of uncertainties on capacity and demand can be evaluated simultaneously through the statistical characteristics of the regression parameters.

Using linear regression equations, the parameter λ, which is the mean of $\ln(S_d/S_c)$, is expressed as a function of PGA:

$$\lambda = A + B\ln(PGA) \qquad (5)$$

In Eq. (5), A and B are the regression coefficients. The standard deviation for the regression is obtained as:

$$\varepsilon = \sqrt{\sum_{i=1}^{n}(y_i - \lambda_i)^2/(n-2)} = \sqrt{S_r/(n-2)} \qquad (6)$$

Where S_r is the sum of squares of the residuals with respect to the regression line for scattered points. The coefficient r^2 gives an indication of the "fit" strength of the regression equation.

In Figure 8, for instance, the linear regression of the column rotation is plotted against PGA for the first damage level of the bridge columns, which corresponds to attaining of the yielding rotation θ_y. This result refers to the accelerogram selection strategy corresponding to the approach A (section 3.3).

The same procedure has been repeated for all damage states, for the two bridge directions (longitudinal and transversal) and for the two approaches (A and B) related to ground motion selection. Figure 9, finally, shows the fragility curves obtained for the longitudinal (a) and transversal direction (b) of the bridge.

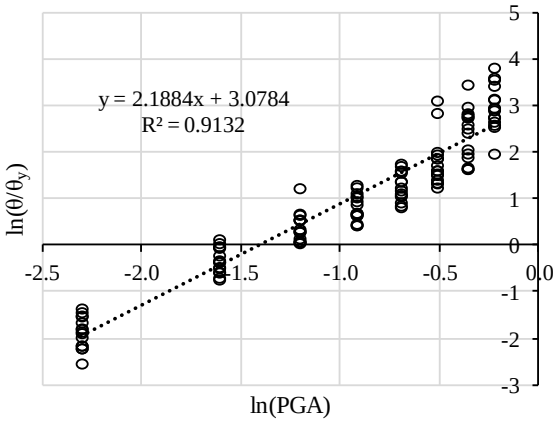

Figure 8. Linear regression analyses of pier rotation θ_y in longitudinal direction with the approach A.

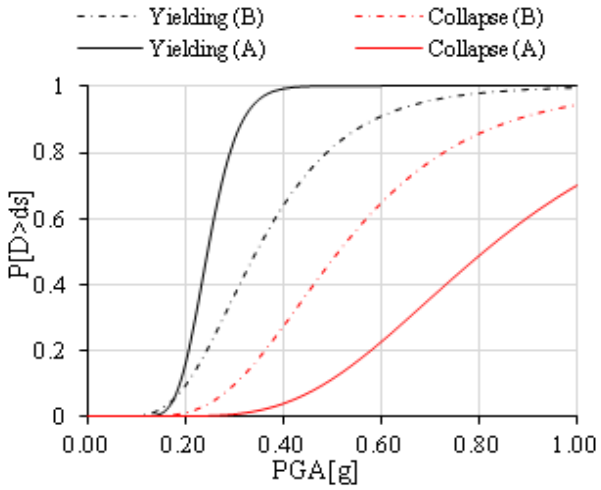

a)

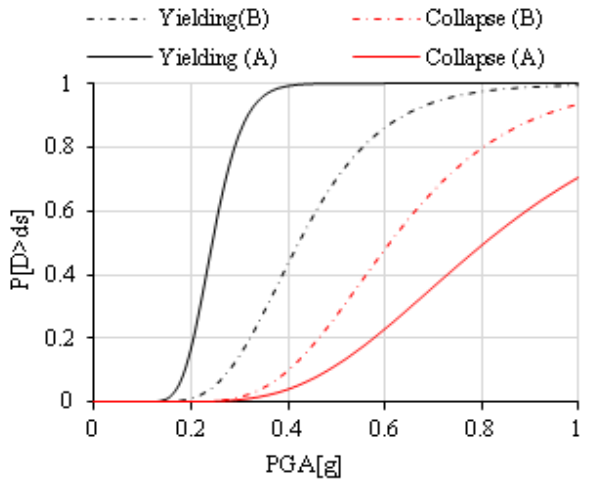

b)

Figure 9. Fragility curves for the bridge pier in longitudinal (a) and transversal (b) direction.

Regardless of the bridge direction, it could be envisaged a strong dependence of the fragility functions on the procedure adopted in selecting the ground motion signals at the base of the bridge pier for a given seismic hazard. With reference to the collapse limit state, the approach B seems much safer while an opposite trend occurs for the yielding limit state. Actually, the responses of the structure at the two limit states get closer because is the soil in dictating the features of the input signals at the pier base and the amount of damping. Therefore, the ground motion computed by specific site response analyses provides an effect similar to a sort of "base isolation", which is beneficial when the structure is in the elastic field (yielding limit state) while it increases the ductility requirements when the structure goes in the post-elastic field.

5 CONCLUSIONS

The paper investigated the effects of seismic site response on the development of analytical fragility curves for reinforced-concrete bridge piers. After a detailed literature review on the state-of-art about fragility function assessment, an application was implemented for the pier of a multi-span simply supported girder bridge, representing a quite common configuration in Italy. Statistical data on structural demand corresponding to peak rock accelerations from 0.1g to 0.8g were generated through structural analysis of several bridge-earthquake pairs. The capacity of the pier was determined from an analytical model. The flexure capacity analyses of the pier were carried out with two different limit states, corresponding to the yielding and collapse conditions respectively, governed by the rotational capacity of the pier at the base. Regardless of the bridge direction (the static scheme is different in longitudinal and transversal direction), a strong dependence of the fragility functions on the procedure adopted in selecting the ground motion signals at the base of the bridge pier was observed. It is worth noting that the input signal obtained by site response analyses makes the responses of the structure at the two limit states closer each other. In particular, the response at the yielding shows a better performance while the one at the ultimate limit state is exacerbated. This outcome suggests, as an interesting perspective of the study, the evaluation of seismic fragility relationships accounting for a complete interaction between the soil and the structure and modelling the bridge piers on a compliant base.

REFERENCES

Agrawal, A.K., Ghosn, M., Alampalli, S., Pan, Y., 2012. Seismic fragility of retrofitted multi-span continuous steel bridges in New York. *ASCE Journal of Bridge Engineering*, **17**, 562–575.

ATC, 1985. Earthquake Damage Evaluation Data for California, *ATC-13*, Applied Technology Council.

Aygun, B., 2011. Efficient Longitudinal Seismic Fragility Assessment of a Multispan Continuous Steel Bridge on Liquefiable Soils, *Journal of bridge Engineering*, ASCE, 2011.

Aygün, B., Dueñas-Osorio, L., Padgett, J. E. and DesRoches, R. (2011). "Efficient longitudinal seismic fragility assessment of a multispan continuous steel bridge on liquefiable soils", Journal of Bridge Engineering, **16**(1): 93-107.

Bardet, J. P., Ichii, K. & Lin, C. H. (2000). EERA a computer program for equivalent-linear earthquake site response analyses of layered soil deposits. Los Angeles, CA, USA: University of Southern California, Department of Civil Engineering.

Basöz, N., Kiremidjian, A., 1998. Evaluation of Bridge Damage Data from the Loma Prieta and Northridge, California Earthquakes, Rep. NO. MCEER 98-0004, Buffalo, N.Y.: Multidisciplinary Center for Earthquake Engineering Research.

Billah, A.H.M.M., Alam, M.S., 2013. Seismic vulnerability assessment of a typical multi-span continuous concrete highway bridge in British Columbia. *Canadian Journal of Civil Engineering*, Manuscript ID: CJCE-2013-0049R2.

Billah, A.H.M.M., Alam, M.S., Bhuiyan, A.R., 2013. Fragility analysis of retrofitted multi-column bridge bent subjected to near fault and far field ground motion. *ASCE Journal of Bridge Engineering*, **18**, 992–1004.

Chaudhary, M., Abe, M., Fujino, Y., 2001. Identification of soil–structure interaction effect in based isolated bridges from earthquake records. *Soil Dynamics and Earthquake Engineering*, **21**, 713–725.

Choi, E., 2002. Seismic analysis and retrofit of mid-America bridges." Ph.D. thesis, Dept. of Civil and Environmental Engineering, Georgia Institute of Technology, Atlanta.

Choi, E., DesRoches, R., Nielson, B., 2004. Seismic fragility of typical bridges in moderate seismic zones. *Eng. Struct*., **26**_2_, 187–199.

Di Laora, R., & de Sanctis, L., 2013. Piles-induced filtering effect on the foundation input motion. *Soil Dyn. Earthquake Engng*, **46**: 52–63.

Elgamal, A., Yan, L., Yang, Z., Conte, J. P., 2008. Three-dimensional seismic response of Humboldt Bay bridge-foundation-ground system, *Journal of Structural Engineering*, **134**(7): 1165-1176.

Fan, K, Gazetas, G, Kaynia, A, Kausel, E, Ahamad, S. 1991. Kinematic seismic response analysis of single piles and pile groups: *J. Geotech. Eng. Div*. **117**(12): 1860-1879.

Gardoni, P., Mosalam, K.M., Der Kiureghian, A., 2003. Probabilistic seismic demand models and fragility estimates for RC bridges. *Journal of Earthquake Engineering*, **7**, 79–106.

Gerolymos, N, Gazetas, G, 2006. Winkler model for lateral response of rigid caisson foundations in linear soil. *Soil Dynamics and Earthquake Engineering*, **26**: 347-361.

González, F., Padrón, L.A., Carbonari, S., Morici, M., Aznárez, J.J., Dezi, F., Leoni, G., 2019. Seismic response of bridge piers on pile groups for different soil damping models and lumped parameter representations of the foundation. *Earthquake Engng Struct Dyn*. 2019; **48**:306–327.

Hwang, H., Liu, J., Chiu, Y., 2001. Seismic fragility analysis of highway bridges. Technical Rep., Center for Earthquake Research and Information, Univ. of Memphis, Memphis, Tenn.

Iervolino, I., Galasso C., Cosenza E., 2009. REXEL: computer aided record selection for code-based seismic structural analysis. *Bulletin of Earthquake Engineering*, **8**:339-362.

Jeremić, B., Jie, G., Preisig, M., Tafazzoli, N., 2009. Time domain simulation of soil-foundation-structure interaction in non-uniform soils, *Earthquake Engineering and Structural Dynamics*, **38**: 699-718.

Kappos, A.J., Panagopoulos, G., Panagiotopoulos, C., Penelis, G., 2006. A Hybrid Method for the Vulnerability Assessment of R/C and URM Buildings. *Bulletin of Earthquake Engineering*, **4**, 391-413.

Karim, K.R., Yamazaki, F., 2003. A simplified method of constructing fragility curves for highway bridges. *Earthquake Engineering and Structural Dynamics*, **32**, 1603–1626.

Kaundinya, I., Heimbecher, F., 2011. Identification and Classification of European Bridge and Tunnel Types. *IABSE–IASS Symposium, London, September 20–23*.

Kwon, O.S., Elnashai, A.S., 2010. Fragility analysis of a highway over-crossing bridge with consideration of soil–structure interactions. Structure and Infrastructure Engineering, **6**, 159–178.

Mackie, K., Stojadinovic, B., 2001. Probabilistic seismic demand model for California highway bridges. *ASCE Journal of Bridge Engineering*, **6**, 468–480.

Mander, J.B., Baso¨z, N., 1999. Seismic fragility curves theory for highway bridges. *In Proceedings of the 5th US Conference on Lifeline Earthquake Engineering*, pp. 31–40: ASCE.

Morici, M., Minnucci, L., Carbonari, S., Dezi, F., Leoni, G., 2019. Simple formulas for estimating a lumped parameter model to reproduce impedances of end-bearing pile foundations. *Soil Dynamics and Earthquake Engineering*, Volume **121**, 2019, Pages 341-355.

Mucciacciaro, M, Gerolymos, N; Sica, S, 2018. Caisson foundations: key aspects and procedure in 3d f. e. m. modeling. *16th European Conference of Earth Eng.* Thessaloniki.

Mwafy, A., Kwon, O., Elnashai, A, 2010. Seismic assessment of an existing non seismically designed major bridge-abutment- foundation system, *Engineering Structure*, **32**: 2192-2209.

Padgett, J.E., DesRoches, R., 2006. Bridge Damage functionality Using Expert Opinion Survey, 8th National Conference on Earthquake Engineering, Earthquake Engineering Research Institute, SanFrancisco, Calif.

Pan, Y., Agrawal, A. K., Ghosn, M., Alampalli, S., 2010. Seismic fragility of multi-span simply supported steel highway bridges in New York state. I: Bridge modeling, parametric analysis and retrofit design. *J. Bridge Eng.* **15**_5_, 448–461.

Pan, Y., Agrawal, A.K., Ghosn, M., 2007. Seismic Fragility of Continuous Steel Highway Bridges in New York State, *Journal of Bridge Engineering*, **12**(6): 689–699.

Ramanathan, K., 2012. Next generation seismic fragility curves for California bridges incorporating the evolution in seismic design philosophy, Ph.D. Dissertation. Georgia Institute of Technology, Atlanta, GA.

Rossetto, T., Elnashai, A, 2003. Derivation of Vulnerability Functions for European-Type RC Structures Based on Observational Data. *Engineering Structures*, **25**, 1241-1263.

Saadeghvaziri, M. A., Yazdani-Motlagh, A. R., Rashidi, S., 2000. Effects of soil structure interaction on longitudinal seismic response of MSSS bridges, *Soil Dynamics and Earthquake Engineering*, **20**: 231-242.

Seed H.B. and Idriss I.M. Soil moduli and damping factors for dynamic response analyses. UCB/EERC-70/10, Earthquake Engineering Research Center, University of California, Berkeley, 1970

Shinozuka, M., Banerjee, S., 2005. Damage Modeling of Reinforced Concrete Bridges, *Tri-Center Meeting on Transportation Networks*.

Shinozuka, M., Feng, M.Q., Lee, J., Naganuma, T., 2000. Statistical analysis of fragility curves. *J. Eng. Mech*., **126**_12_, 1224– 1231.

Stefanidou, S., Markogiannaki, O., Karatzetzou, A., 2018. Fragility Curves for As Built and Retrofitted Bridges Considering Soil Structure Interaction. *16th European conference on Earthquake engineering*. Thessaloniki,2018.

Stefanidou, S.P., Kappos, A.J., 2013. Optimum selection of retrofit measures for R/C Bridges using fragility curves. In M. Papadrakakis, V. Papadopoulos, & V. Plevris (Eds.), *Proceedings of 3rd ECCOMAS Thematic Conference on Computational Methods in Structural Dynamics and Earthquake Engineering (COMPDYN2011)*. Greece: Kos Island 12–14 June 2013, 18 pp.

Tavares, D.H., Padgett, J.E., Paultre, P., 2012. Fragility curves of typical as-built highway bridges in eastern Canada. *Engineering Structures*, **40**, 107–118.

Yamazaki, F., Hamada, T., Motoyama, H., Yamauchi, H., 1999. Earthquake damage assessment of expressway bridges in Japan. *Technical council on lifeline earthquake engineering monograph*, Vol. **16**, ASCE, Reston, Va., 361–370.

Vucetic M., Dobry R. Effect of soil plasticity on cyclic response. *Journal of Geotechnical Engineering* 1991; **117** (1):89-107

Zong, X., 2015. Seismic Fragility Analysis for Highway Bridges with Consideration of Soil-Structure Interaction and Deterioration. CUNY Academic Works.